https://doi.org/10.5194/tc-2022-57
Preprint. Discussion started: 5 April 2022

The Cryosphere Discussions

Comparing rain-on-snow representation across different observational methods and a regional climate model

Hannah Vickers[1], Priscilla A. Mooney[1], Eirik Malnes[1], Hanna Lee[1,2]

[1]NORCE Norwegian Research Centre AS, Postboks 22 Nygårdstangen, 5838 Bergen, Norway
[2]Department of Biology, Norwegian University of Science and Technology (NTNU), Trondheim, Norway

Correspondence to: Hannah Vickers (havi@norceresearch.no)

Abstract. Rain on snow events (ROS) have the potential to cause wide-ranging ecological and societal impacts. Current knowledge and understanding of ROS and their future development are dependent on both observational and model datasets. However, different types of data provide insights into different aspects of ROS and carry limitations that may lead to contrasting results and conclusions, which need to be understood. This study examines the similarities and differences in ROS frequency over mainland Norway, estimated using a regional climate model (Weather Research and Forecasting (WRF)), a remote sensing method (Synthetic Aperture Radar (SAR)), and a gridded observational method (seNorge). Similarities in the geographical occurrence of ROS were obtained from both the WRF model and seNorge, with highest ROS frequency located predominantly along the western and southern coastal regions from autumn through to early spring, but greater ROS activity in the WRF model over inland mountainous areas during late spring and summer. We found significant differences in the spatial occurrence of ROS detected using the remote sensing approach, with much fewer ROS occurrences along the western coast but many more events inland from late autumn through to spring. Ground observations indicated the WRF model has an average accuracy for ROS detection of > 80% for the period studied due to a high rate of detection of non-ROS days and low rate of false positives. However, the WRF model also missed on average >50% of the ROS days detected in ground-based data. For the SAR datasets, both the correct detection and false detection of ROS days was greater, producing a lower overall accuracy of 50-60%. On the other hand, the timing of wet snow occurrence detected by SAR agreed qualitatively well with the onset of ROS detected from ground-based data, but the overall duration of a ROS event was frequently overestimated by SAR due to the persistence of liquid water in the snowpack. The similarities and differences across modelling and observational datasets shown in our study suggests that cross data validation is necessary and there is a need to analyse data collected at a much greater number of sites and future studies should take this into account.

1 Introduction

At present, the occurrence of rain-on-snow (ROS) events has been predominantly confined to high latitude and high-altitude regions where there exists both perennial and seasonal snow cover. Knowledge of the spatial and temporal occurrence of ROS events is highly important due to their wide-ranging implications for nature and society. These include for example flooding, increased avalanche risk in mountainous areas (Eckerstorfer and Christiansen, 2012; Abermann et al., 2019), icing and damage to vegetation (Bjerke et al., 2014) which impact food availability and increased mortality of reindeer populations (e.g., Hansen et al., 2011; Hansen et al., 2014; Forbes et al., 2016), increased soil temperature and permafrost degradation (Westermann et al., 2011). Moreover, there is a pressing need to investigate how ROS events will evolve in an ongoing warming climate, to assist decision makers with risk preparedness and management associated with potential future impacts of ROS.

https://doi.org/10.5194/tc-2022-57
Preprint. Discussion started: 5 April 2022

Regional climate model (RCM) simulations can provide future changes in ROS events under the current projections of climate change at the spatial scale that is relevant for quantifying ecological and societal impacts (e.g., Mooney and Li, 2021). The occurrence of ROS events can be inferred using for example RCM output or observations of meteorological variables. The approach used to detect ROS using these datasets is usually based on thresholding temperature, precipitation, and snow cover data, such that only days where precipitation falling as rain on an existing snowpack, of some minimum extent and depth qualify as ROS days. Modelling studies, however, are based on assumptions that ROS is well represented and simulated based on observations.

Satellite-based remote sensing methods can provide large scale observations of ROS events. For instance, Synthetic Aperture Radar (SAR) is an active microwave sensor that has been widely implemented in many wet snow mapping applications (e.g., Baghdadi et al., 1997; Nagler and Rott, 2000; Malnes and Guneriussen, 2002; Luojus et al., 2007; Nagler et al., 2016, Karbou et al., 2021). SAR is based on the sensitivity of microwave radar sensors to the presence of liquid water in the snowpack, which causes a strong attenuation of the backscattered radar signal. Hence, the detection of wet snow can be taken as a proxy for snowmelt events when the radar signal falls below a given threshold. However, a challenge associated with using remote sensing observation to detect snowmelt caused by a ROS event, is the uncertainty surrounding the amount of liquid water content (LWC) contained in the snowpack that causes the backscattered radar signal to drop to below the threshold commonly used for detection of wet snow. How much LWC in the snowpack is required to produce this drop in the backscattered SAR signal is influenced by several factors including land cover type, surface roughness, incidence angle of the transmitted wave and heterogeneity within the snowpack due to layers of different snow density. All of these can potentially increase or decrease the backscattered radar signal, even if no liquid water is present.

The definition of a ROS event is dependent on the method by which ROS is observed or detected in different datasets. This may lead to erroneous conclusions especially when evaluating model performance and should be considered when comparing outcomes of different ROS studies that have been carried out using different methods of detection. In recent years, forecasting and projecting future ROS events using climate models have been increasingly important to better quantify the upcoming risks under a changing climate. In this study we select Norway as a test case based on 1) the availability of data and 2) the region is a known hotspot of ROS events (Cohen et al. 2015). While there has been both ground-based observations (Pall et al., 2019) and RCM (Mooney and Li, 2021) based studies of past ROS climatology in Norway, there has been no SAR based study for comparison. This study therefore aims to compare ROS representations across various observational methods and regional climate model simulations to create a more robust basis to understand and model future changes in ROS.

The objective of this study is to examine the similarities and differences in ROS frequency over mainland Norway, estimated using a regional climate model (Weather Research and Forecasting (WRF)), a remote sensing method (Synthetic Aperture Radar (SAR)), and a gridded observational method (seNorge). We use the Sentinel-1 SAR remote sensing dataset, by making use of its sensitivity to liquid water, in addition to two model datasets to which the Pall et al. (2019) approach is applied, to identify ROS. Our focus area is mainland Norway, where complex terrain can make it challenging to model and

https://doi.org/10.5194/tc-2022-57
Preprint. Discussion started: 5 April 2022

observe meteorological parameters accurately. Moreover, due to the orbital path of the Sentinel-1 satellites, higher latitude regions such as Norway are imaged more frequently than at mid- or low latitude regions and thus benefit from better temporal resolution. We derive ROS activity from SAR wet snow maps and compare these to ROS activity detected using the "seNorge" gridded observational data of temperature precipitation, snow-covered area (SCA) and snow water equivalent (SWE) (Lussana et al., 2019). Further, we apply the same methods of detection for the gridded observational data to RCM output from the Weather Research and Forecasting (WRF) model (Mooney and Li, 2021) and examine the similarities and differences between the two model datasets as well as between the remote sensing and model detections. Since there is no temporal overlap between the WRF dataset, for 1996-2005 and the Sentinel-1 SAR dataset (2016-2020), the seNorge dataset is compared with the SAR and WRF detections separately. Furthermore, we compare the remote sensing and model-based ROS detections with an additional seNorge product of modelled liquid water content and establish the degree to which the accuracy of the ROS detections is controlled by the level of LWC in the snowpack. While we use Norway as a test case based on various data availability, the methods and framework used in this study can be applied to other snow-covered regions globally.

2 Datasets and Methods

2.1 WRF dataset

The high-resolution regional climate model data used in this study is described in detail in Mooney et al (2020) which also contains a comprehensive evaluation of the simulations. Here, we describe only details that are pertinent to this study and the reader is referred Mooney et al. (2020) for additional details. The model data is produced using Version 3.9.1.1 of the Weather Research and Forecasting (WRF; Skamarock et al. 2019) model. Boundary and initial conditions for the WRF model were obtained from the European Centre for Medium Range Weather Forecasting Interim Reanalysis (ERA-Interim). The simulated data covers the 10-year period 1996–2005. The model setup uses one-way nesting to downscale the ERA-Interim data (grid spacing of ~ 80km) over the Scandinavian Peninsula to 3 km grid spacings. The topography of the study area is illustrated on the WRF data grid in Figure 1.

https://doi.org/10.5194/tc-2022-57
Preprint. Discussion started: 5 April 2022

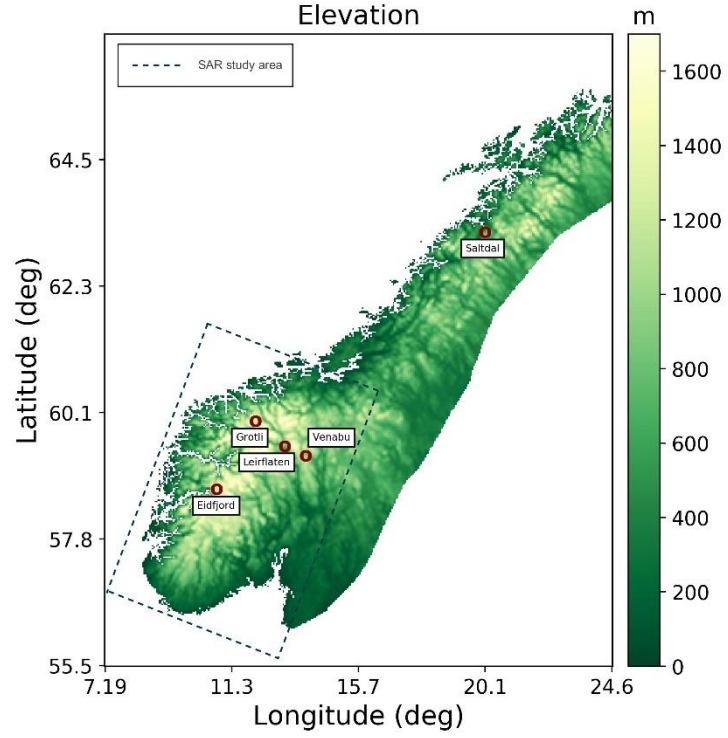

Figure 1. Digital Elevation Model (DEM) for mainland Norway illustrated on the WRF grid and the locations of the meteorological stations where ground-based data have been obtained. The SAR study area over Southern Norway is indicated by the dashed box

2.2 Sentinel-1 dataset

Sentinel-1 is a C-band SAR imaging mission made up of two polar-orbiting satellites, Sentinel-1A, launched in April 2014 and Sentinel-1B, which was launched in April 2016 and has several acquisition modes. Sentinel-1 has been used for studying spring snowmelt and melt dynamics (Marin et al., 2020), wet snow mapping (e.g., Nagler et al., 2016) as well as wet- and dry snow mapping (Tsai et al., 2019; Varade et al., 2019) and may therefore lend itself equally well to tracking snowmelt linked to ROS events, at a much higher spatial resolution than that offered by RCMs. This is especially advantageous in mountainous regions where there are large topographic variations over relatively small (sub-kilometre) distances and where ground-based measurements are often sparse. The existence of ground-based measurements, climate model and remote sensing datasets provides an excellent opportunity to combine cross-disciplinary observations for better definition of ROS types (e.g., Bieniek et al., 2018) and meet the need for improved understanding of ROS in terms of their frequency, seasonality, and intensity (Serreze et al., 2021).

This study makes use of the Interferometric-wide (IW) swath mode which has a swath width of 250 km and nominal pixel spacing of 10 m. The repeat time for identical image geometry is currently 6 days for each satellite. Since the satellites have a polar orbit, mainland Norway is observed with multiple viewing geometries. We use the S1 IW ground-range detected

https://doi.org/10.5194/tc-2022-57
Preprint. Discussion started: 5 April 2022

(GRD) product with co- ("VV") and cross- ("VH") polarizations, and pixels are aggregated to a spacing of 100 m to reduce noise. The SAR backscatter images have been processed for Southern Norway (Figure 1 inset) to produce daily wet snow maps using the Nagler and Rott (2016) approach. The method utilises backscatter from both VV and VH polarizations and a weighting to the contributions is applied to represent an incident angle correction. This adjustment is needed since co-polarized backscatter from wet snow increases at low incidence angles, which produces a smaller backscatter difference between snow-free ground and wet snow, making the detection of wet snow less reliable. SAR image pixels are classified by applying a threshold to the difference between the SAR backscatter and its reference value. These reference values are produced for each sensor and geometry by calculating the average radar backscatter per pixel, based on data acquired in the period November 1st - April 30th during which snow condition is assumed to be dry. While the latter end of this period may include snow that is not dry, the impact of this is expected to be small, since only the 50-percentile is averaged.

Sentinel-1 coverage over southern Norway during the first few years of operation was typically poorer, and different imaging geometries did not cover all areas with the same frequency i.e., some areas of the study region suffer poorer temporal coverage than others. Figure A1 illustrates the difference in image coverage over the study area for the winters (November – April inclusive) 2016/2017 and 2018/2019. For the winter 2016/2017 the area was typically covered by only 10-25 images over the 6-month period, whereas for the winter 2018/2019 there was 60-100 images over most of southern Norway. To produce a time series with daily wet snow maps, these data gaps were addressed by temporal interpolation techniques. For each pixel detected as wet snow followed by a period without SAR acquisitions, it is assumed that the pixel continues to be wet until a new detection of wet or dry snow changes the snow status. This interpolation scheme is sub-optimal for the detection of transient events such as ROS events but is nevertheless needed to compile a complete wet snow time-series that can be compared with model simulations. Due to the irregular temporal sampling in southern Norway (4 samples in 2 days followed by 4 days without samples in the 6-day sampling cycle), the greatest overestimate of wet snow would result in 4 wet snow days instead of 1 day. As such an additional product is generated for the wet snow maps which indicate the "age" of the pixel classification. This value represents the number of days since the last acquisition and therefore provides an estimate of the temporal uncertainty associated with the classification. This product is utilised for ROS detection using SAR by excluding days where the classification age is greater than 2 days, and this is described in greater detail in section 2.5.

2.3 seNorge dataset

seNorge is a gridded observational dataset for mainland Norway produced by the Norwegian Meteorological Institute (MET Norway). The dataset is produced at a grid spacing of 1 km for total daily precipitation, as well as daily mean, maximum and minimum temperature. Several versions of the seNorge have been produced, either as historical data is added to the time series of measurements or when updates are made to the analysis methods. This study makes use of the latest version, seNorge_2018, version 20.05 which covers the period from 1957 to 2019. The seNorge dataset is based on a network of station observations, which are interpolated using two different statistical interpolation methods for temperature and precipitation, respectively. At each grid cell, the result is a weighted average of nearest observations; it is the density of these

https://doi.org/10.5194/tc-2022-57
Preprint. Discussion started: 5 April 2022

observations that controls the effective resolution of the data, with data dense regions producing the highest possible effective resolution and vice versa. This means that in particularly data sparse regions, the effective resolution may be lower than 1 km, even though the measurements are produced on a 1 km grid. The spatial interpolations methods implemented adapts the optimal interpolation (OI) methods automatically based on the local station density. The precipitation dataset is also corrected for wind-induced undercatch and utilises monthly precipitation totals which are dynamically downscaled from global reanalysis data using a regional climate model. In addition, wind measurements derived from a numerical weather model are used.

The seNorge snow model (Saloranta, 2016), uses the gridded temperature and precipitation datasets as input forcing. Solid and liquid precipitation fractions are partitioned using a threshold on temperature, where solid precipitation occurs when air temperature is ≤ 0.5 °C. An extended degree-day model is used to simulate snow and ice melt and SWE and SCA are estimated based on a collection of daily melt rates observed by the Norwegian snow pillow network (Saloranta, 2014). Snow is assumed to be uniformly distributed within the grid cells, and new snow is permitted to form over a uniformly distributed 'old' snowpack. The sub-grid snow distribution reduces the grid cell average melting rates such that they are closer to the late melt season rates. In addition, a seNorge product for liquid water content (LWC) is generated using an operational hydrological model run by the Norwegian Water and Energy Directorate (NVE). This is a calibrated degree-day model based on the seNorge gridded input of precipitation and temperature. This study uses the daily product sampled to 1 km resolution.

2.4 Ground based meteorological observations

Measurements of temperature, total precipitation and snow depth made at five different meteorological stations located within the study area were downloaded from the Norwegian Climate Service Centre (www.seklima.met.no). These sites were chosen based on the completeness of the time series for the three parameters required. For the WRF period (1996-2005), data were obtained for the sites Sauda, Venabu and Eidfjord, while for the SAR period (2016-2020), meteorological data were acquired for the sites Ørskog, Sauda and Grotli. The locations of these sites are illustrated in Figure 1. ROS days were detected in the ground-based measurements by applying the same thresholds to temperature and precipitation measurements as was used on the model and gridded observational datasets (Sect. 2.5). Since the ground-based observations do not include SCA and SWE, a threshold of 2 cm was applied to the snow depth measurements to define a minimum snow cover required for ROS events. In Sect. 3.3, ROS days detected by the WRF model and SAR dataset are compared to the ROS days detected by the ground-based measurements for a single winter. A comparison is not made for the seNorge dataset since the ground-based observations are used in creating the seNorge gridded dataset and would therefore be biased toward a higher accuracy when comparing with ground-based data.

2.5 Detection of ROS days

For the detection and mapping of ROS days using the gridded observational (seNorge) and model (WRF) datasets, the criteria for ROS as defined by Pall et al. (2019) was applied to the temperature, precipitation, SWE and SCA output. ROS

https://doi.org/10.5194/tc-2022-57
Preprint. Discussion started: 5 April 2022

days are detected when daily precipitation as rain exceeds 5 mm, SWE is greater than 3 mm and SCA is at least 25 %. A temperature threshold of 0.5°C was applied to partition precipitation falling as rain or snow. The number of ROS days was counted per month per year of each dataset, after which the monthly mean ROS days for the dataset period was calculated. For the Sentinel-1 daily wet snow maps, ROS pixels were identified as a transition from dry to wet snow classification. The number of ROS days was counted as the number of consecutive days with wet snow following a dry to wet snow transition until the pixel was transitioned to either dry snow or bare ground again. A limitation of this definition is that transitions from dry to wet snow not associated with ROS events may (e.g., weather events with warm air without precipitation) may be detected. On the other hand, a conservative approach was taken to account for the temporal uncertainty associated with pixel classifications made on days without observations, since the method for producing the daily wet snow maps assumes that the snow condition during periods without observations is the same as at the last observation. Therefore, only days where the preceding observation, or SAR acquisition occurred less than 2 days prior were used in the count of consecutive wet snow days following the detection of a ROS event. This rule was implemented to reduce the risk of overestimating the number of ROS days during periods with sparse data coverage. An upper limit of 20 days was applied to the number of consecutive days for a single ROS event to eliminate the possibility of detecting wet snow days following spring snowmelt as a ROS event. It is therefore expected that SAR will under-detect ROS days during spring and summer months when the snowpack has transformed, and the snow condition is continuously wet and very few or no transitions from dry to wet snow occur.

For the comparisons of the ROS maps derived from each dataset, the higher resolution dataset was resampled to the same resolution and grid projection as the lower resolution dataset. That is to say, the seNorge datasets were re-projected to the WRF grid for detection and comparison of ROS days, while the 100 m SAR dataset was resampled to the seNorge resolution (1 km) before the ROS detection algorithm was applied to the SAR images. An evaluation of the accuracy of the WRF and SAR detections have been estimated by calculating the errors of commission and omission, as well as the ROS days and non-ROS days that were correctly identified with respect to the total number of ROS days detected by ground-based data (true positive rate). The error of commission (false positive rate, FP) represents ROS days that were detected by the model data but not by the ground-based data, and the error of omission (false negative rate, FN) therefore corresponds to ROS days detected in the ground-based data but were missed by the model data. The true negative rate (TN) represents the non-ROS days that were detected by both datasets. The overall accuracy then reflects the proportion of correctly detected ROS and non-ROS days and is given by the expression,

$$Accuracy = \frac{TP+TN}{TP+FP+TN+FN} \quad (1)$$

To estimate the accuracy of the SAR approach, a ROS day was defined as when the wet snow fraction time series within a 5 km box, centred on the meteorological stations (Ørskog, Sauda, Grotli) exceeded 15% and this threshold was used to define TP, FP, FN, and TP to estimate the accuracy.

https://doi.org/10.5194/tc-2022-57
Preprint. Discussion started: 5 April 2022

3 Results

3.1 WRF-seNorge comparisons, 1996-2005

The mean days with ROS per month simulated by the WRF model is shown in Figure 2. Geographically, ROS occurs most frequently along the western and southern coasts of Norway between November and March, with the most impacted areas experiencing up to approximately 6 days per month. There is little or no activity in the northern coastal and inland areas of the country. During late spring (April-May), ROS activity no longer occurs predominantly in coastal and low elevation regions, but also further east over inland and mountainous areas, as well as stretching further north along the coast. This is expected as both inland and Arctic areas further north are typically colder during the autumn and winter months. However, an increase in both day- and night-time temperatures in the spring months increases the likelihood of precipitation falling as rain, even in the northernmost and higher elevation regions. By May there are no longer any ROS occurrences in the easternmost parts of Norway, and this is likely due to a disappearance of snow cover from these areas. This pattern continues in June, where the main ROS days are restricted to the mountainous areas, both in the southern, central, and northern parts of Norway. Fewest ROS days are experienced in July, August, and September, which is due to the gradual disappearance of seasonal snow.

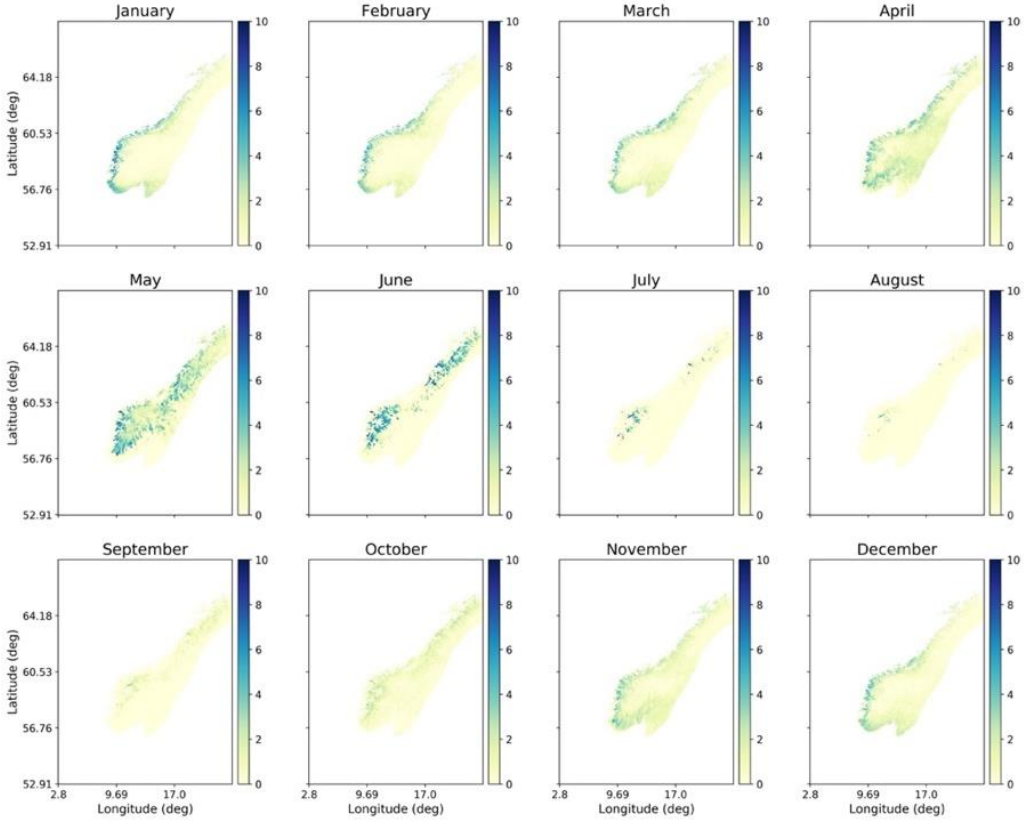

Figure 2. Monthly mean ROS days derived from the WRF model output for the period 1996-2005

https://doi.org/10.5194/tc-2022-57
Preprint. Discussion started: 5 April 2022

225 The geographical pattern of ROS occurrence detected from the seNorge gridded observational dataset (Figure 3) for the autumn and winter months (November to March) is similar to that observed by the WRF dataset. However, the absolute values of ROS frequency are higher in the seNorge detections compared with the WRF model. These differences, illustrated in Figure 4, show that from December through April, the seNorge dataset produces in the region of 1-3 more ROS days along the coastal areas. However, in May and June the seNorge dataset also produces fewer ROS days inland compared with
230 WRF, but there remains a greater number of ROS days in the seNorge dataset along the western coast and further north close to the border with Sweden. For July and August, when ROS is detected only in the mountainous regions inland, the differences between the datasets are small; but during autumn (September - November) the seNorge dataset produces fewer ROS days along the coastal areas compared with WRF, which is the opposite of that observed during the winter and spring months. However, it should be emphasised that the differences are small during September, October, and November, with
235 the seNorge data estimating typically only 1-2 fewer ROS days per month compared with WRF.

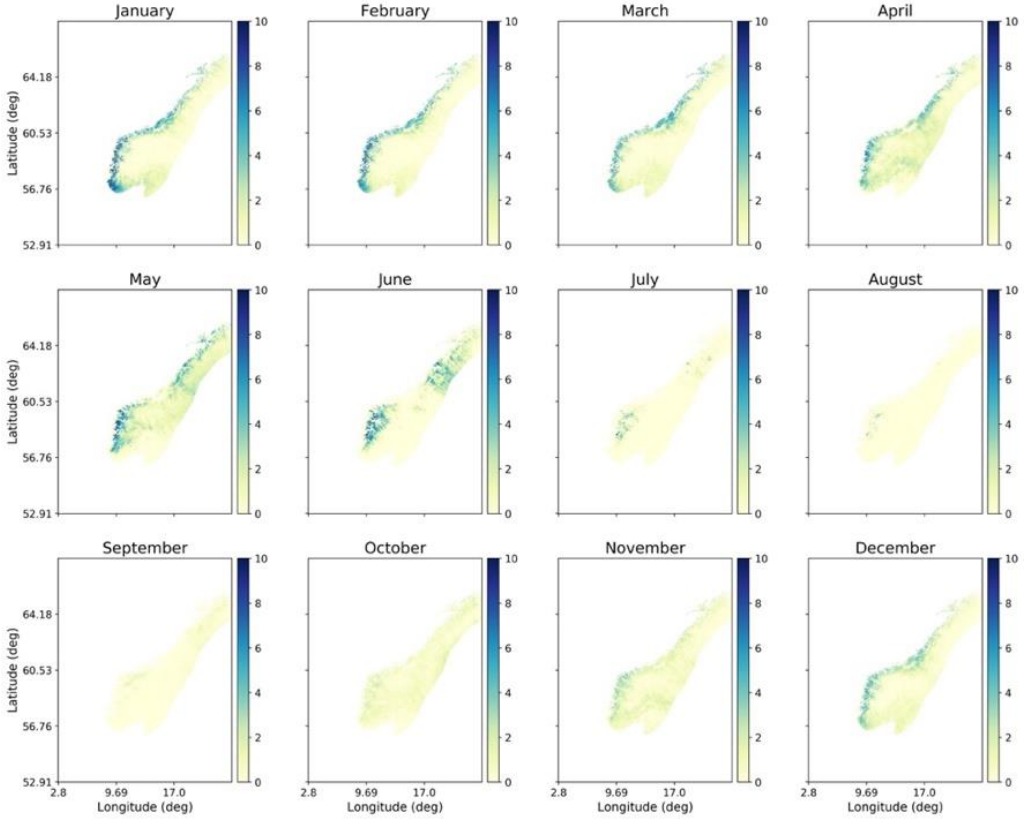

Figure 3. Monthly mean ROS days derived using the seNorge dataset for the period 1996-2005

https://doi.org/10.5194/tc-2022-57
Preprint. Discussion started: 5 April 2022

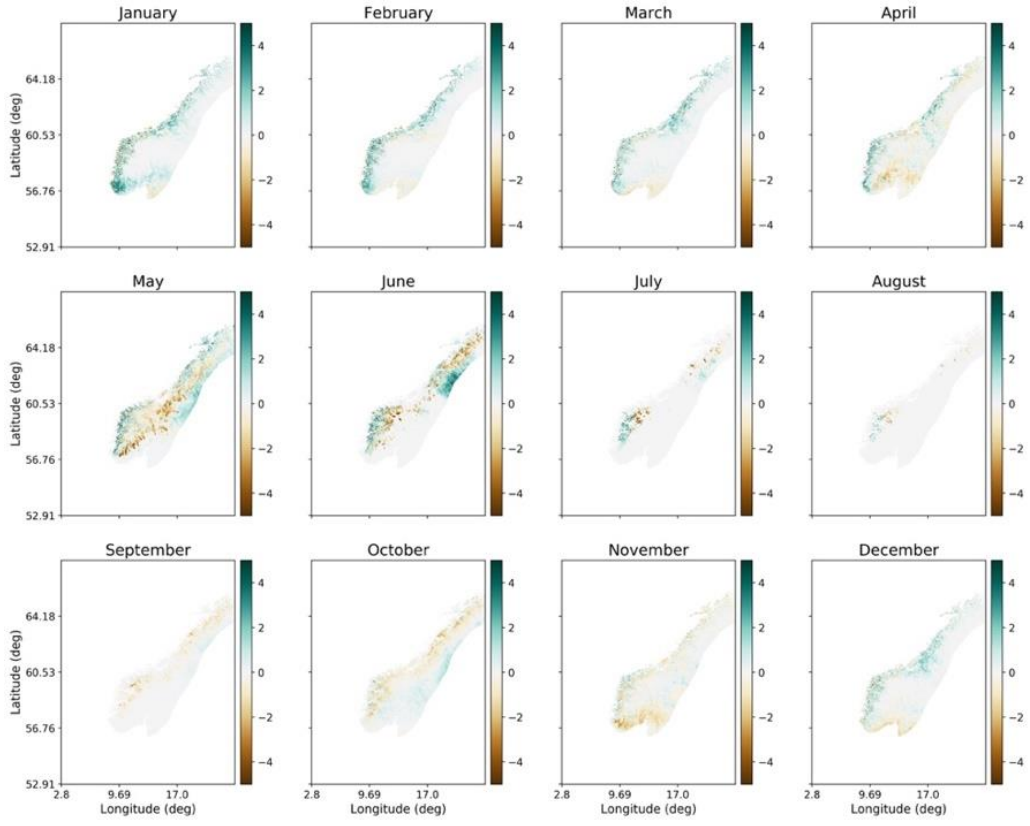

Figure 4. Difference in the monthly mean ROS days between seNorge and WRF model maps for the period 1996-2005. Green areas indicate more ROS days detected by the seNorge dataset; brown areas represent more ROS days detected in the WRF dataset.

3.2 SAR-seNorge comparisons, 2016-2020

The geographical distribution of monthly mean ROS days detected using the remote sensing approach (Figure 5) is very different to the results acquired using the two model datasets, presented in Sect. 3.1, and this is the case for all months. Whereas ROS activity is confined to the western and southern coastal areas during the winter months in both the seNorge gridded observational and WRF model datasets, ROS detections derived from the SAR wet snow maps are distributed across most of the study area, including large parts of the inland areas. There are no distinct ROS "hotspots" evident in the SAR maps, and the areas with most ROS days varies from month to month. ROS activity declines after April, and ROS days in May are confined to areas further inland from the western coast. As expected, there is almost no ROS detected during the summer and early autumn months (June-September inclusive) since any remaining snow cover, which is confined to mountainous areas, will be continually wet and no dry-to-wet snow transitions occur. During October, ROS is found in the central parts of the study area, away from the coast, but spreads both eastwards and southwards by November.

https://doi.org/10.5194/tc-2022-57
Preprint. Discussion started: 5 April 2022

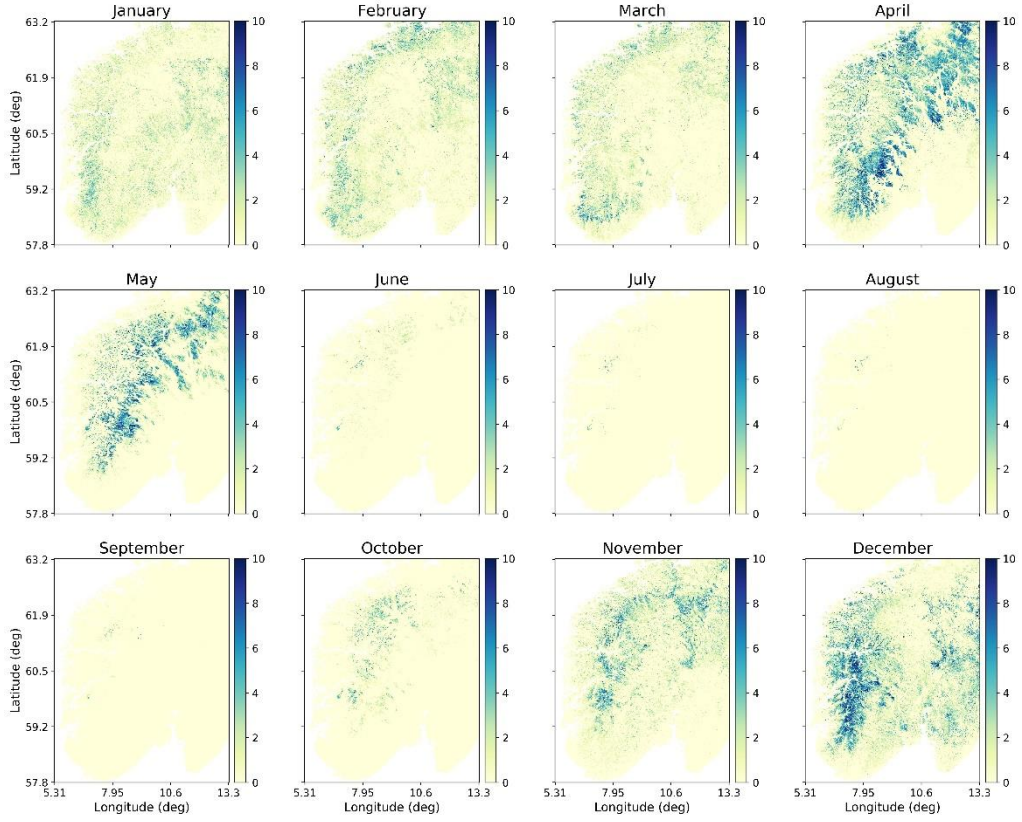

Figure 5. Monthly mean ROS days derived using the Sentinel-1 SAR wet snow maps for the period 2016-2020

The seNorge ROS detections for the SAR period (2016-2020) indicates similar geographical patterns of ROS as for the earlier model period, with most ROS days occurring along the western coast during the winter and spring months but being confined to inland mountainous areas during the summer months. However, for the 2016-2020 period, fewest ROS days during the winter months was detected in February in the gridded observational dataset. Furthermore, there is slightly increased ROS days further inland from the coast during December for the 2016-2020 period compared with the 1996-2005 period. The main differences between the gridded observational and remote sensing detections (Figure 6) are that the gridded observational data produces greater ROS activity along the western coast during the late autumn, winter, and spring months, while more ROS are detected by remote sensing over inland areas. The largest differences between the two datasets exceeded ± 5 ROS days.

https://doi.org/10.5194/tc-2022-57
Preprint. Discussion started: 5 April 2022

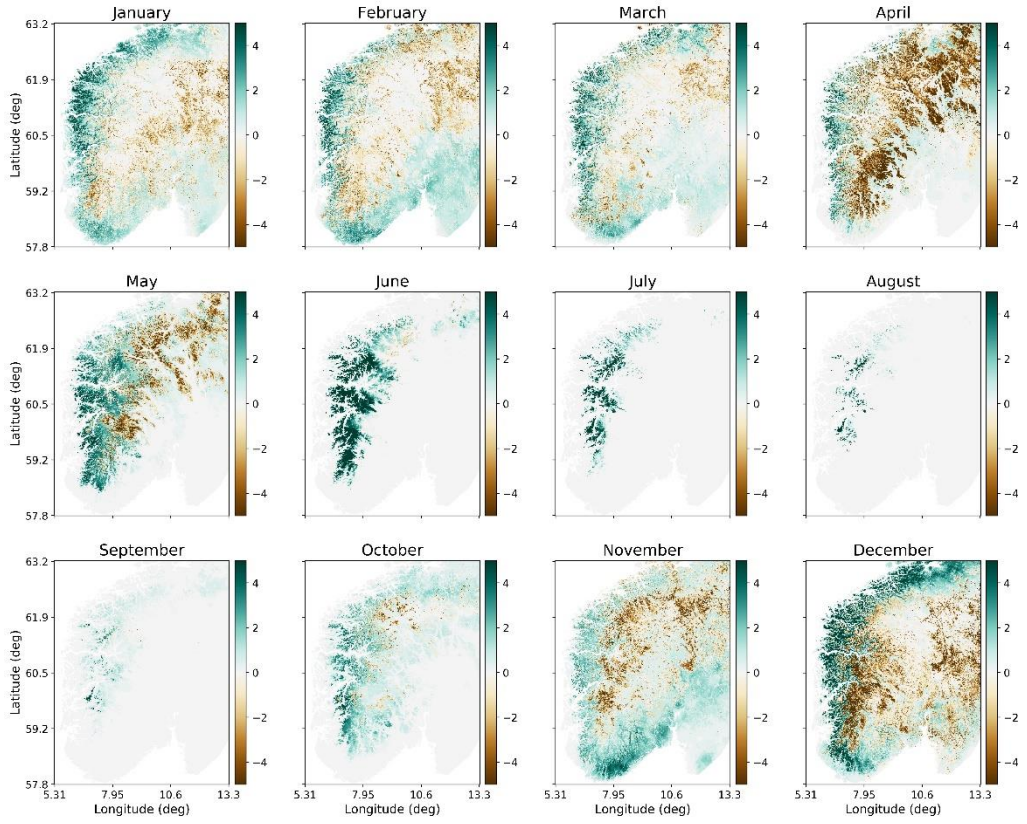

Figure 6. Difference in the monthly mean ROS days (SeNorge – SAR) for the period 2016-2019. Green areas indicate more ROS days detected by the seNorge dataset and brown areas correspond to more ROS days in the SAR dataset.

3.3 Comparison with ground-based data

Data from the (WRF) model and ground-based stations are compared for the winter 1999-2000 in Figure 7. ROS days are detected as outlined in Sect. 2.4 and 2.5 for the ground-based and model data, respectively. It should also be re-emphasised that the simulated ROS events from WRF reflect data corresponding to a 3 km x 3 km grid cell, while the ground-based measurements are made at specific locations, such that the spatial validity of the two detections is not entirely the same.

During this winter, the lower elevation stations Sauda (5 m.a.s.l) and Eidfjord (117 m.a.s.l) experience frequent episodes of rain between the beginning of December and the start of April, while at the higher elevation station Venabu (930 m.a.s.l) almost no days with total daily precipitation >5 mm falling as rain was registered in the ground-based measurements, except for one day close to the end of April. However, while the model data correctly predicts no ROS days between December and the end of March, there were however several days in both November and April where ROS was detected by the model but not in the ground-based data. This is also true for the Sauda and Eidfjord observations, where several false ROS detections were made by the model in November (and April at Sauda). However, it can also be seen that the model ROS detections

https://doi.org/10.5194/tc-2022-57
Preprint. Discussion started: 5 April 2022

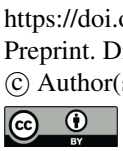

agree qualitatively well with the ground-based ROS detections between December and March, even though several false and missed ROS detections, are present in the time series at these stations.

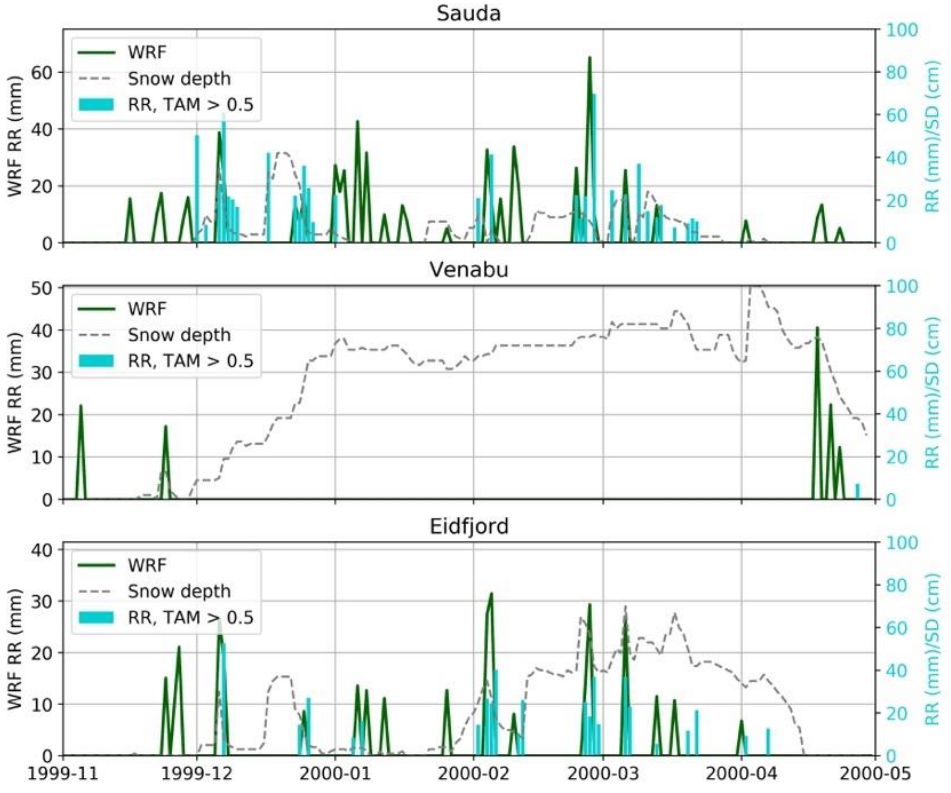

Figure 7: Comparison of ROS precipitation detected by the WRF model (dark green) compared with ROS precipitation detected by the ground-based meteorological data (light blue) for the winter season 1999/2000 for three sites; Sauda (5 m.a.s.l.), Eidfjord (117 m.a.s.l.) and Venabu (930 m.a.s.l.). Also shown are the ground-based snow depth measurements (black, dashed line). Only precipitation on days detected as ROS events are shown.

Figure 8 shows data compared for ROS events detected at Ørskog and Grotli for the 2016-2017 winter season using the gridded observational and ground-based measurements (a,b) and the SAR wet snow fraction and LWC measurements (c, d). These sites were selected due to the contrasting elevations, with Ørskog (5 m.a.s.l.) located close to sea level while Grotli is located at mountain elevation (872 m.a.s.l.). For Ørskog, there were three ROS events detected in the gridded observational dataset, even though there were in total seven episodes of ROS detected using the ground-based data. The episodes detected by the seNorge data coincide with short-lived spikes in LWC with maximum values of 10 %. The snow depth decreased to 0 cm following all ROS events detected in the meteorological data. Spikes of approximately 70 % wet snow fraction are visible during November and March in the remote sensing dataset. These increases in wet snow fraction do not coincide with increased LWC or ROS events detected using ground-based data. For the three ROS days in March where ROS was detected in ground-based data, there was also increased wet snow fraction (> 20 %). These events in March 2017 were neither detected by the gridded observational dataset, nor were there any increases in the associated LWC data.

https://doi.org/10.5194/tc-2022-57
Preprint. Discussion started: 5 April 2022

At Grotli, there was a total of seven ROS days detected using the gridded observational dataset. However, only four of these days also correlated with ROS detections in the ground-based measurements. There is also high LWC following all seven of these ROS events, but a slight delay between the onset of the ROS event and the peak in LWC is apparent. LWC decreases slowly over the course of days to weeks after the peak in LWC coinciding with the ROS event, and the rate of decrease in LWC is not correlated with the absolute amount of precipitation. There is a qualitatively good relationship with between the timing of the peaks in wet snow fraction and LWC, but like LWC, the wet snow fraction does not decrease immediately once a ROS event has stopped, but instead decreases over the course of several days or not at all, as is the case for the ROS days in early December 2016 and April 2017. It is the persistence of wet snow detection following the end of a ROS event that is likely to be the source of high false positive rates at this site. For all peaks in wet snow fraction, the LWC is also at a maximum (10%), even though the wet snow fraction peaks vary in magnitude.

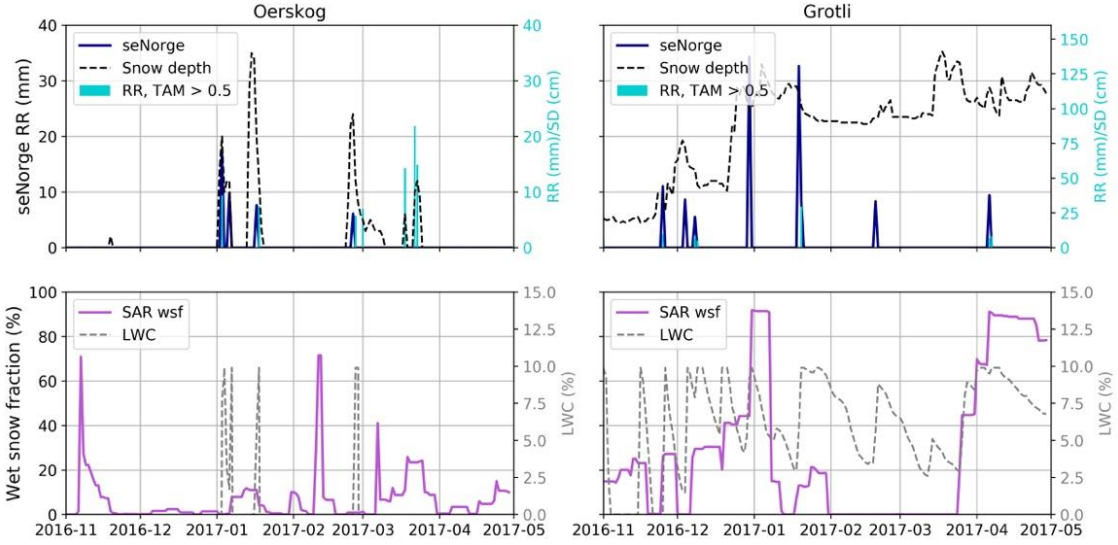

Figure 8: Comparison of ROS day precipitation measured by ground-based observations (light blue) and seNorge (dark blue) and snow depth (black, dashed) at Ørskog (a) and Grotli (b); SAR wet snow fraction ("SAR wsf", light purple) and seNorge LWC measurements (grey, dashed) for the winter season 2016/2017 at Ørskog (c) and Grotli (d).

The errors of omission and commission for both the model and remote sensing detections are calculated for all winter seasons in the dataset and given as the mean of all years in Table 1. The WRF model had the highest rate of correct ROS detections at Sauda (43.1%), but also the highest false positive rate (13.5%). However, while the true positive rate was low at all three stations, the false positive rate is also much lower than the true positive rate, indicating that while the model in general misses many ROS days detected by the ground-based data, it also does not over-detect ROS to a great extent either. This is also reflected in the high true negative rates at all three stations. In contrast, the accuracy metrics comparing the wet snow fractions with the detected ROS days from ground-based data reveal that the true positive rate is on average for the period, satisfactory at Grotli (74.2 %) but the mean false positive rate is also much higher (51.2 %) than the false positive rates for the WRF model. At Grotli, the mean false positive rate is > 60% of the true positive rate, whereas for the WRF

https://doi.org/10.5194/tc-2022-57
Preprint. Discussion started: 5 April 2022

model, the mean false positive rate was typically 25-30% of the true positive rate. A similar result is clear at both Ørskog and Sauda, where the false positive rate is at least as high as the true positive rate (Sauda) or close to 80% of the true positive rate, leading to an overall accuracy of between 50 and 60% at all stations where a comparison against ground-based data was made. In contrast, the WRF model, despite simulating < 50% of all ground-based ROS events, produced higher accuracy scores due to a low false positive rate and high rate of non-ROS days, with an accuracy of > 80% at all stations.

WRF	TP (%)	FP (%)	FN (%)	TN (%)	Accuracy (%)
Sauda	43.1	13.5	56.9	86.5	82.0
Venabu	0	1.05	100	98.4	98.5
Eidfjord	26.8	6.4	73.2	93.6	87.7
SAR	TP (%)	FP (%)	FN (%)	TN (%)	Accuracy (%)
Ørskog	51.7	38.5	48.3	61.5	60.8
Sauda	41.8	42.2	58.2	57.8	57.0
Grotli	74.2	51.2	25.7	48.8	48.8

Table 1. True positive, false positive, false negative and true negative rates for the WRF model and SAR detections, validated against ground-based ROS detections derived using the meteorological station measurements. Rates have been calculated for each winter (1 November – 30 April) and averaged over all years in the WRF period (1996-2005) and SAR study period (2016-2020)

4 Discussion

This study investigated the differences across WRF model and observations in order to provide a better evaluation of the model as well as an evaluation of the remote sensing data such as the SAR detection approach.

Both the model and gridded datasets reproduced a similar geographical occurrence of ROS, where ROS is most frequent along the western and southern coastal areas of Norway during winter and early spring but confined to inland mountainous areas during summer where there is still an existing seasonal snow cover. These geographical patterns are observed and well described in earlier studies (Pall et al., 2019; Mooney and Li, 2021). On the other hand, we found that the gridded observational dataset estimates fewer ROS days than the model dataset during autumn (September - November) but tends to produce slightly more ROS days along the western and southern coasts in the winter and spring months. This could be interpreted in several ways, as a difference in rainfall between the two datasets or a difference in snow cover where rain is falling. A comparison of snow-covered area (SCA) produced using seNorge observations and the Moderate Resolution Imaging Spectroradiometer (MODIS) instrument for Svalbard showed that seNorge underestimates SCA with respect to MODIS during the autumn months but estimates slightly higher SCA than MODIS during the spring months (Vickers et al., 2021). Although the study area was focused on Svalbard, the results may also be representative of the seNorge dataset for mainland Norway, thereby partly explaining the differences in ROS distributions observed here.

https://doi.org/10.5194/tc-2022-57
Preprint. Discussion started: 5 April 2022

There were significant differences in the geographical patterns of ROS detected using the SAR remote sensing approach when compared with the ROS detections from the gridded observations. There were a greater number of ROS days detected across inland areas during late autumn, winter, and spring months in the remote sensing dataset, but no ROS detected during the summer months. This difference occurs because during the summer months when seasonal snow is continuously wet, there is no transition from dry to wet snow that can be detected by SAR. Moreover, SAR cannot distinguish whether liquid water presence in the snowpack is due to snowmelt caused by warmer air temperatures, or rainfall. We therefore expect that a considerable proportion of the ROS days detected across inland areas in the remote sensing data could in fact simply represent snowmelt events resulting from warmer air. The apparent lack of ROS detections along the western coast in the remote sensing dataset could be attributed to the exclusion of ROS events where the detected duration was greater than 20 days. Here, there may be incidences of ROS events that result in the presence of wet snow persisting for longer than this threshold, and as such several ROS events may have been discounted. Increasing this threshold may therefore improve ROS representation by SAR in these regions, when compared with the gridded observations. Furthermore, there are uncertainties linked to the distribution of observations used by the seNorge model. Observations are typically biased, with a denser network in densely populated areas compared with mountainous areas and a greater number of observations in the west of the study area compared with further east. There is also a similar south-north bias in the number of stations (Lussana et al., 2019). This produces a greater uncertainty in the interpolation methods of the data-sparse regions. It is in these inland mountainous regions that we observed the greatest differences between seNorge and the SAR detections of ROS, with seNorge typically detecting most ROS days along the west coast during the winter and early spring months where the observation network is also denser.

Comparisons of the WRF model-detected ROS days with ground-based observations revealed that the model does not simulate all the ROS days observed by the ground-based data, but does not tend to over predict ROS either, as reflected by the relatively low false positive rate. However, the ground-based data consists of three parameters necessary to identify ROS (temperature, precipitation, snow depth), whereas the Pall et al. (2019) criteria was applied to four parameters (temperature, precipitation, snow covered area and snow water equivalent), thereby acting as a stricter filter on which days could be identified as ROS days. This may have contributed to the lower true positive rate of the simulated ROS days when compared with ground-based data. In contrast, the SAR approach produced both higher true positive rates and false positive rates compared with the model, resulting in lower overall accuracy, which was on average, approximately 55%. This contrasts with the mean accuracy of the model detections which was > 90%.

This work demonstrates that there exist similarities as well as differences in ROS representation between both regional climate models, hybrid observation-model datasets and remote sensing datasets. Differences are not only reflected in the spatial distributions of ROS but also in the number of ROS days. Moreover, comparisons with ground-based observations also revealed both strengths and weaknesses in the ability of both model-based and remote sensing approaches to detect ROS events in Norway. Most model evaluation studies use observational products to evaluate the model's performance without consideration of observational uncertainties and limitations (Poschlod et al., 2018; Kotlarski et al., 2014). However, this

https://doi.org/10.5194/tc-2022-57
Preprint. Discussion started: 5 April 2022

work has shown that it is important to consider this to avoid incorrect conclusions about model performance. The results of this study therefore highlight the importance of making cross comparisons across different types of observations to evaluate the suitability of different products in representing ROS occurrence. Ultimately, there is a need for high quality datasets that can serve as ground truthing.

5 Conclusion

Rain-on-snow events are becoming of increasing importance to understand due to their wide-ranging impacts on both nature and society. Mapping the occurrence of ROS in both space and time is performed differently when using either model or observational datasets, which may also lead to contrasting results. Understanding the method of detection as well as uncertainties associated with datasets that are used for evaluation of the ROS detections is crucial in order to draw informed conclusions concerning the accuracy of the results. We have cross-compared ROS representations from model, remote sensing, and ground-based observations to gain a better understanding of the similarities and differences between the different approaches, as well as evaluate the representation of ROS events provided by the WRF model.

Whilst a qualitatively good correspondence between the timing of peaks in both LWC and SAR wet snow fraction was observed together with the onset of ROS detected using ground-based observations at high elevation sites, both LWC and wet snow fraction decreased gradually following ROS events. As a result, the number of days with wet snow following the onset of a ROS event was typically much greater than the actual number of days with precipitation. Therefore, the sensitivity of SAR to liquid water in the snowpack, as well as gaps in data acquisition makes the SAR remote sensing approach currently less well suited to estimating the duration of ROS events using the approach presented in this study. Moreover, the remote sensing approach to detecting ROS events has not been widely tested in terms of different climatic zones with different land cover types. It is therefore recommended that future work should test the SAR approach in different snow-covered environments worldwide to determine which factors produce the best or worst performance of the method.

We were not able to make a direct comparison between the regional climate model and remote sensing approaches in this study due to lack of temporal and spatial overlap between the datasets. But, by comparing both datasets with a gridded observational dataset which was common to both datasets, we found most spatial similarities in ROS representation between the model and gridded observations, with ROS occurrence dominating along the west and southern coastal areas during winter and early spring months. It is therefore expected that there would be similar spatial differences between the model and remote sensing data, as was found for the comparisons between the gridded observations and remote sensing dataset. This comparison indicated that the ROS events occurred much more frequently over inland areas using the remote sensing method, when compared with gridded observations. A major challenge in evaluating the performance of both model and remote sensing detections of ROS was the lack of ground observations with complete time series of daily mean air temperature, precipitation, and snow depth. Data gaps, or only two of the three required parameters being measured at many of the meteorological stations meant that time series of ROS occurrence could not be produced at many sites using the ROS

https://doi.org/10.5194/tc-2022-57
Preprint. Discussion started: 5 April 2022

410 criteria required. This severely limits the possibility for performing a thorough evaluation of the different datasets. There is therefore a need to analyse data collected at a much greater number of sites and future studies should address this.

Appendix

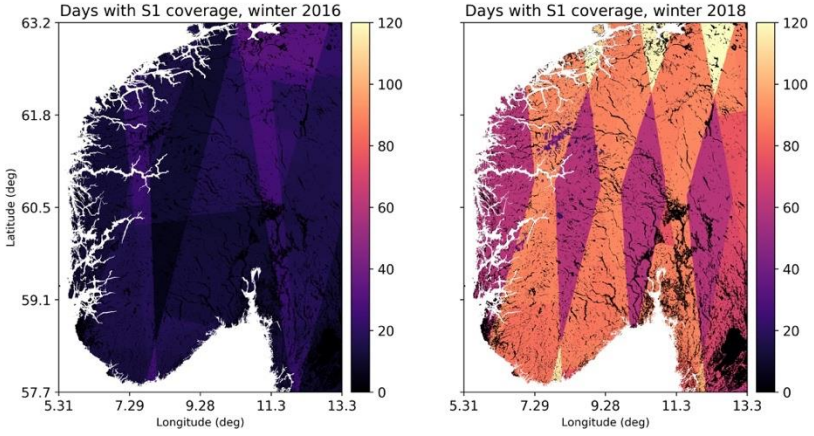

415 **Figure A1: (left) Number of Sentinel-1 images per pixel for winter 2016 (November 2015-April 2016) and (right) image coverage for winter 2018. Data coverage for 2018 was typically 4 times greater than in 2016**

Data availability:

seNorge temperature dataset: Cristian Lussana (2020). seNorge_2018 daily mean temperature 1957-2019 (20.05) [Data set]. Zenodo. https://doi.org/10.5281/zenodo.3923706

seNorge precipitation dataset: Cristian Lussana (2020). seNorge_2018 daily total precipitation amount 1957-2019 (20.05) 420 [Data set]. Zenodo. https://doi.org/10.5281/zenodo.3923703

The seNorge liquid water content product is available at www.senorge.no under the snow wetness layer

The WRF and SAR datasets are available upon request.

Author contribution: HV, HL, and PAM conceptualized the study, HV analysed the datasets, PAM provided the WRF data, 425 EM provided the SAR and LWC datasets. All authors contributed to writing the manuscript.

Competing interests:

The authors declare that they have no conflict of interest

Acknowledgements:

Simulations were performed on resources provided by UNINETT Sigma2—the National Infrastructure for High Performance Computing and Data Storage in Norway (NN9280K, NN9486K, NN8002K, NS8002K, NS9599K). This work was in part supported by the Research Council of Norway Grants (#309625 PRISM; #301777 FRONTIER). P. A. M. and H.L. was partially supported by the European Union's Horizon 2020 research and innovation framework programme under Grant agreement no. 101003590 (PolarRES).

References

Abermann, J., Eckerstorfer, M., Malnes, E., Hansen, B.U.: A large wet snow avalanche cycle in West Greenland quantified using remote sensing and in situ observations, Nat Hazards 97, 517–534. https://doi.org/10.1007/s11069-019-03655-8 , 2019

Baghdadi, N.: Capability of Multitemporal ERS-1 SAR Data for Wet-Snow Mapping, Remote Sensing of Environment 60, 174–186. https://doi.org/10.1016/S0034-4257(96)00180-0 , 1997

Bieniek, P. A., Bhatt, U. S., Walsh, J. E., Lader, R., Griffith, B., Roach, J. K., Thoman, R. L.: Assessment of Alaska Rain-on-snow events using dynamical downscaling, J. Appl. Meteorol. Climatol. 57, 1847–63, 2018

Bjerke, J.W., Rune Karlsen, S., Arild Høgda, K., Malnes, E., Jepsen, J.U., Lovibond, S., Vikhamar-Schuler, D., Tømmervik, H.: Record-low primary productivity and high plant damage in the Nordic Arctic Region in 2012 caused by multiple weather events and pest outbreaks, Environ. Res. Lett. 9, 084006. https://doi.org/10.1088/1748-9326/9/8/084006 , 2014

Cohen, J., Ye, H., Jones, J.: Trends and variability in rain-on-snow events, Geophys. Res. Lett. 42, 7115– 7122, doi:10.1002/2015GL065320 , 2015

Eckerstorfer, M., Christiansen, H.H.: Meteorology, Topography and Snowpack Conditions causing Two Extreme Mid-Winter Slush and Wet Slab Avalanche Periods in High Arctic Maritime Svalbard: Two Mid-winter Slush and Wet Slab Avalanche Periods in Svalbard, Permafrost and Periglac. Process. 23, 15–25. https://doi.org/10.1002/ppp.734 , 2012

Forbes, B.C., Kumpula, T., Meschtyb, N., Laptander, R., Macias-Fauria, M., Zetterberg, P., Verdonen, M., Skarin, A., Kim, K.-Y., Boisvert, L.N., Stroeve, J.C., Bartsch, A.: Sea ice, rain-on-snow and tundra reindeer nomadism in Arctic Russia, Biol. Lett. 12, 20160466. https://doi.org/10.1098/rsbl.2016.0466 , 2016

Hansen, B.B., Aanes, R., Herfindal, I., Kohler, J., Sæther, B.-E.: Climate, icing, and wild arctic reindeer: past relationships and future prospects, Ecology 92, 1917–1923. https://doi.org/10.1890/11-0095.1 , 2011

Hansen, B.B., Isaksen, K., Benestad, R.E., Kohler, J., Pedersen, Å.Ø., Loe, L.E., Coulson, S.J., Larsen, J.O., Varpe, Ø.: Warmer and wetter winters: characteristics and implications of an extreme weather event in the High Arctic, Environ. Res. Lett. 9, 114021. https://doi.org/10.1088/1748-9326/9/11/114021 , 2014

Karbou, F., Veyssière, G., Coleou, C., Dufour, A., Gouttevin, I., Durand, P., Gascoin, S., Grizonnet, M.: Monitoring Wet Snow Over an Alpine Region Using Sentinel-1 Observations, Remote Sensing 13, 381. https://doi.org/10.3390/rs13030381 , 2021

https://doi.org/10.5194/tc-2022-57
Preprint. Discussion started: 5 April 2022

460 Kotlarski, S., Keuler, K., Christensen, O. B., Colette, A., Déqué, M., Gobiet, A., Goergen, K., Jacob, D., Lüthi, D., van Meijgaard, E., Nikulin, G., Schär, C., Teichmann, C., Vautard, R., Warrach-Sagi, K., and Wulfmeyer, V.: Regional climate modeling on European scales: a joint standard evaluation of the EURO-CORDEX RCM ensemble, Geosci. Model Dev., 7, 1297–1333, https://doi.org/10.5194/gmd-7-1297-2014, 2014.

Luojus, K.P., Pulliainen, J.T., Metsamaki, S.J., Hallikainen, M.T.: Snow-Covered Area Estimation Using Satellite Radar
465 Wide-Swath Images, IEEE Trans. Geosci. Remote Sensing 45, 978–989. https://doi.org/10.1109/TGRS.2006.888864 , 2007

Lussana, C., Tveito, O.E., Dobler, A., Tunheim, K.: seNorge_2018, daily precipitation, and temperature datasets over Norway, Earth Syst. Sci. Data 11, 1531–1551. https://doi.org/10.5194/essd-11-1531-2019, 2019

Malnes, E., Guneriussen, T.: Mapping of snow covered area with Radarsat in Norway, in: IEEE International Geoscience and Remote Sensing Symposium. Presented at the IEEE International Geoscience and Remote Sensing Symposium.
470 IGARSS 2002, IEEE, Toronto, Ont., Canada, pp. 683–685. https://doi.org/10.1109/IGARSS.2002.1025145 , 2002

Marin, C., Bertoldi, G., Premier, V., Callegari, M., Brida, C., Hürkamp, K., Tschiersch, J., Zebisch, M., Notarnicola, C.: Use of Sentinel-1 radar observations to evaluate snowmelt dynamics in alpine regions, The Cryosphere 14, 935–956. https://doi.org/10.5194/tc-14-935-2020 , 2020

Mooney, P.A., Li, L.: Near future changes to rain-on-snow events in Norway, Environ. Res. Lett. 16, 064039.
475 https://doi.org/10.1088/1748-9326/abfdeb , 2021

Mooney, P.A., Sobolowski, S., Lee, H.: Designing and evaluating regional climate simulations for high latitude land use land cover change studies, Tellus A: Dynamic Meteorology and Oceanography 72, 1–17. https://doi.org/10.1080/16000870.2020.1853437 , 2020

Nagler, T., Rott, H.: Retrieval of wet snow by means of multitemporal SAR data, IEEE Trans. Geosci. Remote Sensing 38,
480 754–765. https://doi.org/10.1109/36.842004 , 2000

Nagler, T., Rott, H., Ripper, E., Bippus, G., Hetzenecker, M.: Advancements for Snowmelt Monitoring by Means of Sentinel-1 SAR, Remote Sensing 8, 348. https://doi.org/10.3390/rs8040348, 2016

Pall, P., Tallaksen, L.M., Stordal, F.: A Climatology of Rain-on-Snow Events for Norway, Journal of Climate 32, 6995–7016. https://doi.org/10.1175/JCLI-D-18-0529.1 , 2019

485 Poschlod, B., Hodnebrog, Ø., Wood, R.R., Alterskjær, K., Ludwig, R., Myhre, G., Sillmann, J.: Comparison and Evaluation of Statistical Rainfall Disaggregation and High-Resolution Dynamical Downscaling over Complex Terrain, Journal of Hydrometeorology 19, 1973–1982. https://doi.org/10.1175/JHM-D-18-0132.1 , 2018

Saloranta, T.M.: Operational snow mapping with simplified data assimilation using the seNorge snow model, Journal of Hydrology 538, 314–325. https://doi.org/10.1016/j.jhydrol.2016.03.061 , 2016

490 Saloranta, T.M.: New version (v.1.1.1) of the seNorge snow model and snow maps for Norway, 2014

Serreze, M.C., Gustafson, J., Barrett, A.P., Druckenmiller, M.L., Fox, S., Voveris, J., Stroeve, J., Sheffield, B., Forbes, B.C., Rasmus, S., Laptander, R., Brook, M., Brubaker, M., Temte, J., McCrystall, M.R., Bartsch, A.: Arctic rain on snow events:

bridging observations to understand environmental and livelihood impacts, Environ. Res. Lett. 16, 105009. https://doi.org/10.1088/1748-9326/ac269b , 2021

Skamarock, W.C., Klemp, J.B., Dudhia, J., Gill, D.O., Liu, Z., Berner, J., Wang, W., Powers, J.G., Duda, M.G., Barker, D.M., Huang, X.-Y.: A Description of the Advanced Research WRF Model Version 4. UCAR/NCAR. https://doi.org/10.5065/1DFH-6P97 , 2019

Tsai, Dietz, Oppelt, Kuenzer: Wet and Dry Snow Detection Using Sentinel-1 SAR Data for Mountainous Areas with a Machine Learning Technique. Remote Sensing 11, 895. https://doi.org/10.3390/rs11080895 , 2019

Varade, D., Dikshit, O., Manickam, S.: Dry/wet snow mapping based on the synergistic use of dual polarimetric SAR and multispectral data, J. Mt. Sci. 16, 1435–1451. https://doi.org/10.1007/s11629-019-5373-3 , 2019

Vickers, H., Malnes, E., van Pelt, W.J.J., Pohjola, V.A., Killie, M.A., Saloranta, T., Karlsen, S.R: A Compilation of Snow Cover Datasets for Svalbard: A Multi-Sensor, Multi-Model Study, Remote Sens. 13, 2002. https://doi.org/10.3390/rs13102002 , 2021

Westermann S., Boike, J., Langer, M., Schuler, T.V., Etzelmüller, B.: Modelling the impact of wintertime rain events on the thermal regime of permafrost, The Cryosphere 5, 945–59, 2011